An Automatic Evaluation Procedure for 3-D Scanners in Robotics Applications

Bent Møller, Ivar Balslev, and Norbert Krüger

***Abstract*— Various 3-D sensors with highly varying properties exist. Comparing these sensors has traditionally been a cumbersome task, involving scanners to be set up and tested at the same place. In this article, a portable test plate, which can be used to test 3-D scanners, is described. Using this portable test plate, eight different scanners have been tested. These are compared both qualitatively and quantitatively.**

***Index Terms*— 3-D measurement devices, benchmark testing, bin picking, robot vision systems.**

I. Introduction

MANY robotic applications require sensor input. In recent years, the development in 3D sensors has contributed to the fact that more such applications now use 3D scanners instead of regular camera images.

However, since several different 3D scanner technologies exist, choosing the optimal 3D scanner for a specific application might not be simple. Also, the choice will always depend on the problem at hand. For example, if 3D data should be used for mobile robot navigation [1], small errors in depth measurements might not be important as opposed to quality control [2], which often requires a very high 3D data quality.

When using 3D scanners, several problems may arise depending on the objects to be scanned. Examples of objects with problematic surfaces can be seen in Fig. 1. The 3D data acquired for this scene using two of the 3D scanners that have been tested can be seen in Fig. 2. The shiny surface of object *A* will lead to large variations in the amount of light that is reflected back to 3D scanners, depending on whether the light emitted by the scanners is reflected directly back to the sensor or in some other direction. This may lead to regions with missing data points as shown for object *A* in Fig. 2. The structured surface of object *B* may lead to small depth variations depending on the scanner technology. Also, because the surface of this object does not exhibit perfect Lambertian reflections, the amount of reflected light will decrease towards the extremal contours, leading to missing points. This is visible in Fig. 2(a). Low amounts of reflected light may also be a problem with object *C*. Again, this is primarily visible in Fig. 2(a).

Fig. 1. Various objects with surfaces which may give problems when using 3-D scanners.

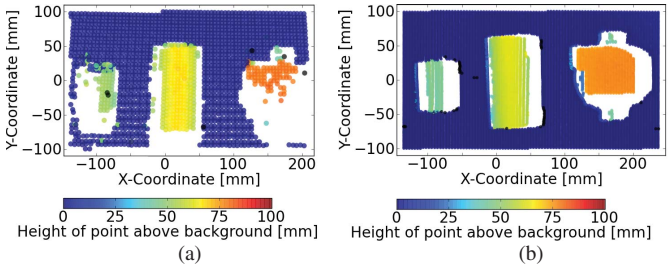

Fig. 2. 3-D data acquired for scene in Fig. 1 using two different 3-D scanners. (a) SCAPE Grid Scanner. (b) SICK Ranger 50E.

To date, there have been made some evaluations of scanners in various application contexts [3]–[12]. For a detailed discussion, see section II.

The quality of the measurement of 3D scanning devices depends on a large number of factors which can be divided into external factors, such as surface reflectance, surface specularity and ambient light intensity, as well as internal properties such as depth resolution, point density and measurement noise. Due to this considerable amount of factors, it is an acknowledged problem to build meaningful and practical devices to evaluate 3D scanners in a generic way, see e.g. [5], [6].

Existing solutions face the problem that they only test some of the characteristics of scanners, e.g. [8], which only tested the performance when scanning marble surfaces and [9], which only tested the performance when scanning various colors.

Manuscript received September 12, 2012; revised October 29, 2012; accepted October 29, 2012. Date of publication November 21, 2012; date of current version January 15, 2013. This work was supported in part by The Danish National Advanced Technology Foundation through the Bin-Picker Project, and the IntellAct Project under Grant FP7-ICT-269959. The associate editor coordinating the review of this paper and approving it for publication was Dr. Subhas C. Mukhopadhyay.

B. Møller is with the University of Southern Denmark, Odense M DK-5230, Denmark, and also with Scape Technologies, Odense C 5000, Denmark (e-mail: bmo@scapetechnologies.com).

I. Balslev is with Scape Technologies, Odense C 5000, Denmark (e-mail: ivb@scapetechnologies.com).

N. Krüger is with the University of Southern Denmark, Odense M DK-5230, Denmark (e-mail: norbert@mmmi.sdu.dk).

Color versions of one or more of the figures in this paper are available online at http://ieeexplore.ieee.org.

Digital Object Identifier 10.1109/JSEN.2012.2228638

(a) (b)

Fig. 3. (a) Front and (b) back of mobile test plate that has been created. Width is approximately 30 cm.

(a) (b) (c) (d) (e) (f) (g) (h)

Fig. 4. Scanners that have been evaluated. (a) SICK Ranger 50E. (b) SICK Scanning Ruler. (c) 3D3 HDI Advance R2. (d) SCAPE Grid Scanner. (e) PMD CamCube 3.0. (f) Fotonic C70. (g) Xbox Kinect. (h) ASUS Xtion PRO.

Also, almost all tests require scanner testing experts to test the scanners, making it an expensive and time-consuming task to test and compare a large range of scanners.

In contrast to existing devices, in this paper we introduce an evaluation device which can be used to test and compare the performance of scanners on a range of different surfaces. Also, this evaluation device is highly mobile, meaning that the acquisition of 3D data of the evaluation device does not have to be performed by the scanner testing experts. Hence, we have been capable of testing a large variety of sensors applicable to indoor applications. The evaluation device that has been developed for this purpose; a small test plate, is shown in Fig. 3.

The focus of the test has been on robotics applications where high quality data of stationary scenes is required, e.g. quality control, object recognition or bin picking. Hence, it has been assumed that all tested 3D scanners could deliver high quality data. We perform tests of the scanners shown in Fig. 4 and provide both qualitative and quantitative results.

The remainder of this article is structured as follows: In section II, an overview of the current state-of-the-art in scanner testing is presented. In section III, we present a brief overview of 3D scanner technologies that have been deemed interesting in the context of robotics applications. This is in section IV followed by a description of the test that has been developed. Results are presented in section V and conclusions are presented in section VI.

II. 3-D Scanner Evaluation Approaches

As previously mentioned, not many tests of 3D scanners have been described so far. These can be divided into two groups. The first group consists of those that test 3D scanners based on scan results of one type of surface only. This includes [7] where three different scanners are tested by scanning a single white flat surface at various distances, [8] where three different scanners are tested by scanning flat marble surfaces and [9] where a single laser scanner is tested by scanning surfaces of varying color. Although these tests uncover particular strengths and weaknesses of the scanners under evaluation, they can not be used to make general statements about the performance of the scanners when scanning a variety of surfaces.

The remaining scanner tests ([3]–[6], [10]–[12]) evaluate one or more scanners each by scanning different surfaces. In [3], a single structured light scanner, the SL2 scanner made by the company XYZRGB, has been tested on a number of different surfaces as well as on some reference objects. However, this test did not include an evaluation of the performance of the scanner on shiny surfaces which, as will be shown in section V, is an important factor if attempting to scan this type of surface.

In [4], six different 3D scanners have been tested. Results for spatial resolution and random depth errors have been included for scans made of a small sugar bowl covered with primer paint. Six different scanners have also been tested in [10] where a portable test rig has been scanned. The tests described in [4], [10] have, however, not included any evaluation of the influence of specular reflections on the scan results. Also, the influence of surface reflectance inhomogeneities has not been evaluated upon for the investigated scanners. But, as will be shown in section V, inhomogeneous surface reflectance will lead to lower 3D data quality than expected for some scanner types. Hence, this factor should not be neglected when testing 3D scanners.

In [5], a single Time-of-Flight sensor mounted on an Automated Guided Vehicle (AGV) has been used to scan surfaces with various surface reflectance and specularity and qualitative results are given. Based on this test, changes to the ANSI/ITSDF B56.5 Safety Standard for Guided Industrial Vehicles were recommended. These recommendations were based on the observation that varying surface reflectance and specularity had a large impact on the scan result, just as will be shown in section V.

Three different 3D scanners have been tested in [6] where the conclusions are based on scans of a flat white matte plate and two different archaeological objects. Again, it is difficult to

make any general statements about the real-world performance of the scanners. This would have required a more extensive test including several additional testing parameters, e.g. sensitivity to variations in surface reflectance and surface specularity.

There has been a thorough survey of laser scanners for use in landscape modeling projects [11] but due to their prices and low scan speeds, they are not considered to be interesting for use in robotics applications as e.g. quality control, object recognition and bin picking. A large portion of the tests that have been performed in [11] use the same ideas as in [12], which shows test results for a range of different 3D scanners. All 3D scanners that have been tested in [12] are, however, also not relevant in the context of robotics applications because of their low scan speeds. Also, all scanner testing using the methods in [11], [12] must be performed by the scanner testing experts. This then implies that in order to test a single 3D scanner, this must be shipped to the scanner testing experts after which they must set it up and perform the test scans in their local environment. If the goal is to test numerous different scanners, this procedure will make scanner testing a very cumbersome task. In contrast, our system does not rely on calibrated reference data, implying that scanning can be performed everywhere while still allowing for scan data to be comparable.

Because of the shortcomings of the test methods presented above, this work has been created in order to be able to test and compare the real-world performance of a number of different 3D scanners.

III. Short Range 3-D Scanner Technologies

This section will provide a short overview of the 3D scanner technologies that have seemed interesting in applications like quality control, object recognition and bin picking.

A. Laser Triangulation Scanners

The principle behind laser triangulation scanners is shown in Fig. 5(a). Here, a laser line is projected onto the surface of the object which is subject to scanning. The displacement of the imaged laser line, which will depend on the distance from the camera to the impact of the laser line, can then be estimated from an image taken by the camera. From this, a single 3D profile of the scene can be determined. However, in order to scan an entire scene, either the laser emitter or the entire camera-laser unit must be rotated or translated while stitching together each single 3D profile generated one after the other. Although the term "Laser triangulation scanner" is most often used for this type of 3D scanner, the light source may be any type of light source emitting a single light sheet, e.g. a LED projector.

There are several different vendors offering triangulation scanners, including SICK, Leutze, ShapeGrabber and LMI Technologies. Common for all these is the fact that the movement of the scanner relative to the scene is the responsibility of the user. One of the tested scanners, the SICK Ranger 50E, is such a standard triangulation scanner. However, SICK will soon release a new scanner [13], which will be referred to as the Scanning Ruler in this work. This scanner handles the movement of the laser line internally, simplifying the use of the scanner. This scanner has also been tested.

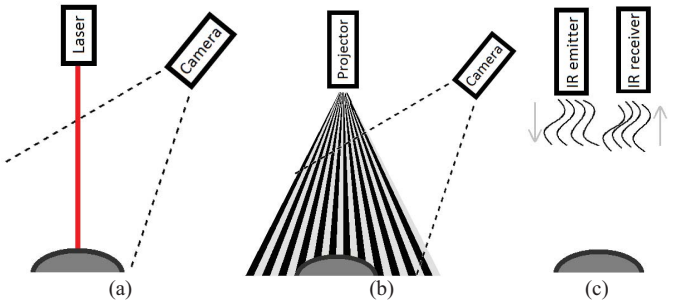

Fig. 5. Principle behind three common 3-D scanner technologies. (a) Laser triangulation. (b) Stripe pattern. (c) Time-of-flight.

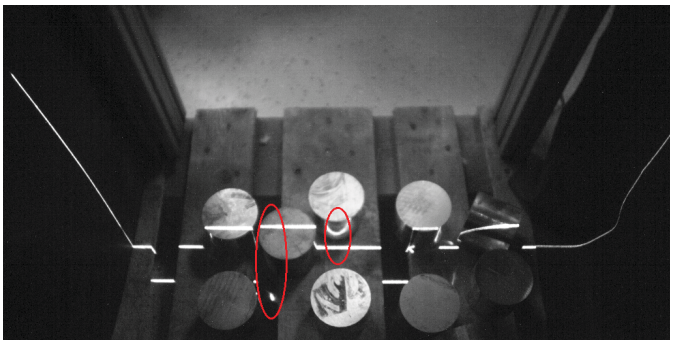

Fig. 6. Issue when using laser triangulation scanners; several matches for the laser line being visible in an image. The brightness of this image has been increased for visualization purposes.

Laser triangulation scanners typically give 3D data with large point densities but suffer from the fact that the scanner must be rotated/translated relative to the scene, making scan times range from one to several seconds, depending on the desired Field of View (FoV).

Also, laser triangulation scanners can be quite sensitive to specular reflections from the scene being scanned. These can be both "double reflections" as seen in the ellipses in Fig. 6, where the laser line is reflected specularly onto another surface from which it is diffusely reflected back to the camera, as well as specular reflections of incoherent light from the laser, reflected straight back to the camera. These issues with specular reflections are then worsened by occlusions, which are due to the base line of the triangulation scanner. Here, the primary diffuse reflection might not be visible in the image, increasing the risk of a false match for the laser line in the image which in turn may lead to outliers in the 3D data.

B. Structured Light Scanners

Principally, structured light scanners are also based on the triangulation principle [14] but instead of only a single laser line being emitted, some structured pattern is emitted onto the surface. Two of the predominant techniques with highly differing characteristics are explained in the following.

1) Stripe Pattern Scanners: These scanners, also called fringe projection scanners, rely on a pattern consisting of high contrast stripes being projected onto the surface of the scene

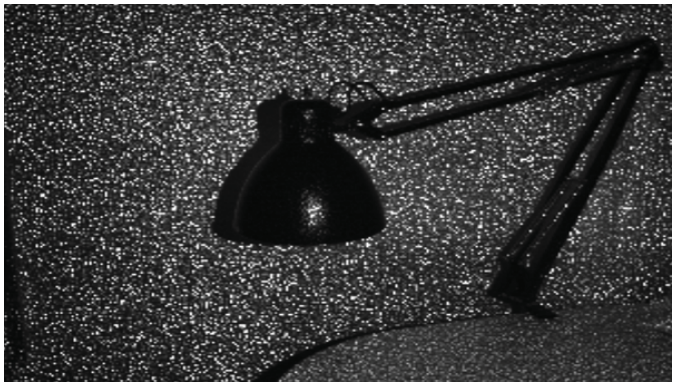

Fig. 7. Sample image of static pattern emitted by ASUS Xtion PRO 3-D scanner.

by a projector. The displacement of the stripes is recorded by a camera. Due to depth ambiguities [14], it is necessary to acquire images of the projection of 6–10 different stripe patterns with varying stripe widths and displacements before being able to derive the complete 3D point cloud of the scene. This then implies that the scene must be static during these image acquisitions which typically last up to a few seconds. This principle is visualized in Fig. 5(b). The HDI Advance R2 by 3D3 solutions, which has been tested, uses this scanning principle.

As will be seen in section V-A.3, this type of scanner may be quite sensitive to ambient light due to the limited power of standard projectors. However, they have the advantage of consisting of very simple hardware components and no movable parts.

2) Static Pattern Scanners: Whereas stripe pattern scanners rely on several images in order to be able to create a point cloud of the entire scene, structured light scanners using static patterns generate point clouds from a single image. This is achieved by making sure that the emitted pattern does not contain structures that might lead to ambiguities when reprojected to the image plane while being used inside the working range of the 3D scanner. An example of such a pattern as seen by the the Asus Xtion PRO 3D sensor is shown in Fig. 7. Since only one image is required per point cloud, these can be generated as quickly as the image can output images, provided that image processing algorithms can keep up with the data stream. For the ASUS Xtion PRO as well as the Xbox Kinect, which is built on the same reference design by PrimeSense, this results in point clouds at a frame rate of 30 Hz when running at full resolution. Another example of a static pattern projector is the SCAPE Grid Scanner[1], which is offered by Scape Technologies as a short range 3D scanner used for bin picking where it is mounted on the tool of the robot. All three static pattern scanners mentioned above have been tested in this work.

Static pattern scanners typically have a fixed working range inside which they must be used. Also, they generally generate less points per point cloud than stripe pattern scanners and laser triangulation scanners. They do, however, have the advantage of high acquisition speeds.

[1]This scanner is based on a method first described in [15]. The fixed pattern is emitted by a LED projector with a photolithographically manufactured mask in front of it.

C. Time-of-Flight Scanners

Instead of being built on the triangulation principle, Time-of-Flight (ToF) sensors measure distances to surfaces by calculating the time it takes a known signal emitted from the sensor to travel to the surface, where it is reflected, and back to the sensor. This principle is shown in Fig. 5(c), where the received signal is phase shifted depending on the distance traveled.

The only kind of ToF scanner that is interesting in the context of this test is ToF cameras due to their speed. For these, a sinusoidal IR signal is emitted from the sensor onto the scene and reflected back to the camera. Here, the reflected signal is captured by a special type of optical sensor similar to a standard CCD chip in a camera. What makes this kind of sensor special is the fact that each single pixel does not only generate an intensity value but also a distance value based on the phase of the incoming IR signal [16].

As will be shown in section V-B, the quality of 3D data from ToF cameras highly depends on the calibration quality. However, even after having performed additional calibrations that take all known systematic errors into account [16]–[18], RMS errors are still significantly higher than for the other sensors considered here. As will also be shown in section V-B, these RMS errors highly depend on the reflectance of the surface being scanned with darker surfaces leading to lower signal to noise ratios, resulting in larger RMS errors. In top of that, ToF cameras suffer from various non-systematic errors that depend on the specific scene being scanned [18].

In this evaluation, two ToF cameras have been included; the PMD CamCube 3.0 and the Fotonic C70.

IV. Defining a Test of 3-D Scanners

As explained in section I, there has previously been no test of the real-world performance of 3D scanners on a range of surfaces, usable in quality control, object recognition and bin picking. This means that the parameters that these scanners must be evaluated upon must be redefined based on those in [3]–[12].

A first requirement to the test is that it should be highly mobile so that scanning can be performed by scanner vendors. Due to this, a small and flat test plate has been created, shown in Fig. 8. This test plate is an approximately 30 cm wide and 5 mm thick acrylic plate and can therefore easily be sent to 3D scanner vendors. On each side of it, a piece of paper laminated with matte laminate has been glued using spray glue.

Looking back at Fig. 1, the structure of surfaces can be seen to influence the quality of 3D data. The reason for this is that an inhomogeneous surface reflectance may lead to a displacement of an emitted signal (laser line etc.) when observed from a camera as explained in [8]. This 2D displacement of an intensity ridge or peak will then lead to a displacement of the resulting 3D point.

How much a scanner is disturbed by inhomogeneous surface reflectance might also depend on the spatial frequency of the

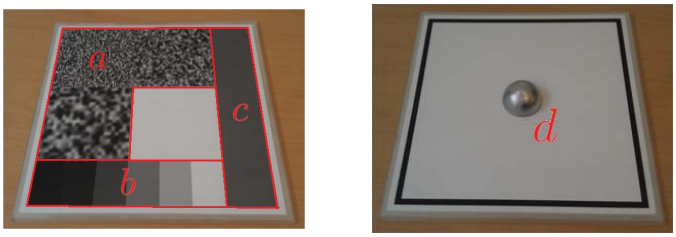

(a) (b)

Fig. 8. (a) Front and (b) back of mobile test plate that has been created with individual regions highlighted.

pattern. Hence, three structured regions, marked by the letter *a*, have been created on the test plate in Fig. 8(a). Looking at the RMS error of points from a plane in these regions will then show which influence the structured regions have on the depth error of 3D points.

Again, looking back at Fig. 1, another issue that 3D scanners might face is too little reflected light from the surface of objects. Therefore, the region *b* has been created on the test plate. Looking at the number of points inside each of the rectangular regions will then show whether the scanners have difficulties acquiring data from all types of surfaces, no matter how bright or dark they are.

Finally, a gray reference region (*c*) has been included in order to determine the performance of the scanner when scanning surfaces of low complexity. This gray region has a reflectivity similar to many metal surfaces.

The back of the test plate has been reserved for determining how reflections affect scanners. Since reflections may influence data quality in large areas around the reflecting surface, depending on the scanning principle, this test could not be included on the other side of the test plate. The specular reflections are created by a plastic hemisphere with a diameter of 5 cm placed in the center of the plate. The hemisphere has been painted with a glossy metallic paint, making specular reflections as dominating as possible. The performance of scanners on this side of the test plate is then evaluated based on the number of points that are acquired on the hemisphere itself as well as the deviations from the actual surface. The errors in circular regions outside the hemisphere will also be evaluated, making it evident whether reflections may lead to depth deviations at other places than the shiny surfaces.

The test explained above is performed for two different levels of ambient light, in order to make explicit which scanners are affected by ambient light. This means that the test plate is scanned at both 140 and 320 lux, resembling conditions ranging from a relatively shielded environment to office lighting.

Depending on the scanner, it may be desirable to test it at a certain distance. In order to minimize the dimensionality of testing parameters, each single scanner is only tested at one distance. This distance is the approximate working distance that would apply to the sensor if it were to be used in a bin picking application, meaning that 3D sensors that are small enough to be placed on the end effector of a robot will be tested at a distance of approximately 60 cm, whereas 3D sensors that are too large for this are tested at a distance of 1.5 m. The latter should approximately match the distance from a 3D sensor mounted above a bin to its contents while leaving space for a working robot between the sensor and the objects.

V. Results

Since the scanners have been divided into two groups based on their size, the results for each of these groups will be given separately in the following. Due to limited space, all results given will, unless otherwise stated, be for scans made at approximately 320 lux ambient light. This is because most test results were unchanged when lowering the amount of ambient light.

First, several qualitative results will be given where the test plate is oriented as shown in Fig. 8. For several scanners, this will also be evident from the local distribution of errors. This is followed by an evaluation of the quantitative results.

A. Large 3-D Sensors

As specified in section IV, large 3D sensors have been testes at a distance of approximately 1.5 m. These include the following three:

1) SICK Ranger 50E: Qualitative results when scanning the test plate using the SICK Ranger 50E 3D camera can be seen in Fig. 9(a). These results are for a setup with a class 2B laser mounted with a base line of 40 cm to the Ranger camera and pointing towards the camera at an angle of 15°. When scanning the front of the test plate, the laser line was parallel to the Y-axis of the test plate which is clearly seen from the large errors where the reflectance of the test plate has a large gradient in the direction of the X-axis. This kind of systematic error is typical to laser triangulation scanners as was explained in section III-A. From visual inspection, these systematic errors are seen to be up to 2 mm. Also, it can be seen how the error of the points increases as the surface of the front of the test plate gets darker in the region marked *b* in Fig. 8.

The results for the back of the test plate show a small region in the center of the shiny hemisphere where the errors are below 1 mm. From there, data becomes less reliable with large errors and outliers being present. Due to the nature of triangulation scanners like this, the shiny hemisphere also leads to outliers in the region outside the hemisphere. Quantitative results are given at the end of this section.

2) SICK Scanning Ruler: Qualitative results when scanning the test plate using the SICK Scanning Ruler can be seen in Fig. 9(b). Just as for the Ranger camera, systematic errors of up to 2 mm are seen at large reflectance gradients of the front of the test plate, only are these at large gradients in the direction of the Y-axis of the test plate. This is because the rotation of the test plate relative to the laser is different from that when the SICK Ranger was tested. Also, it could seem like the random noise in the structured regions is slightly lower than for the Ranger camera in exchange for slightly more dominating systematic errors.

The results for the back of the test plate resemble those for the Ranger except for the fact that outliers and/or false data

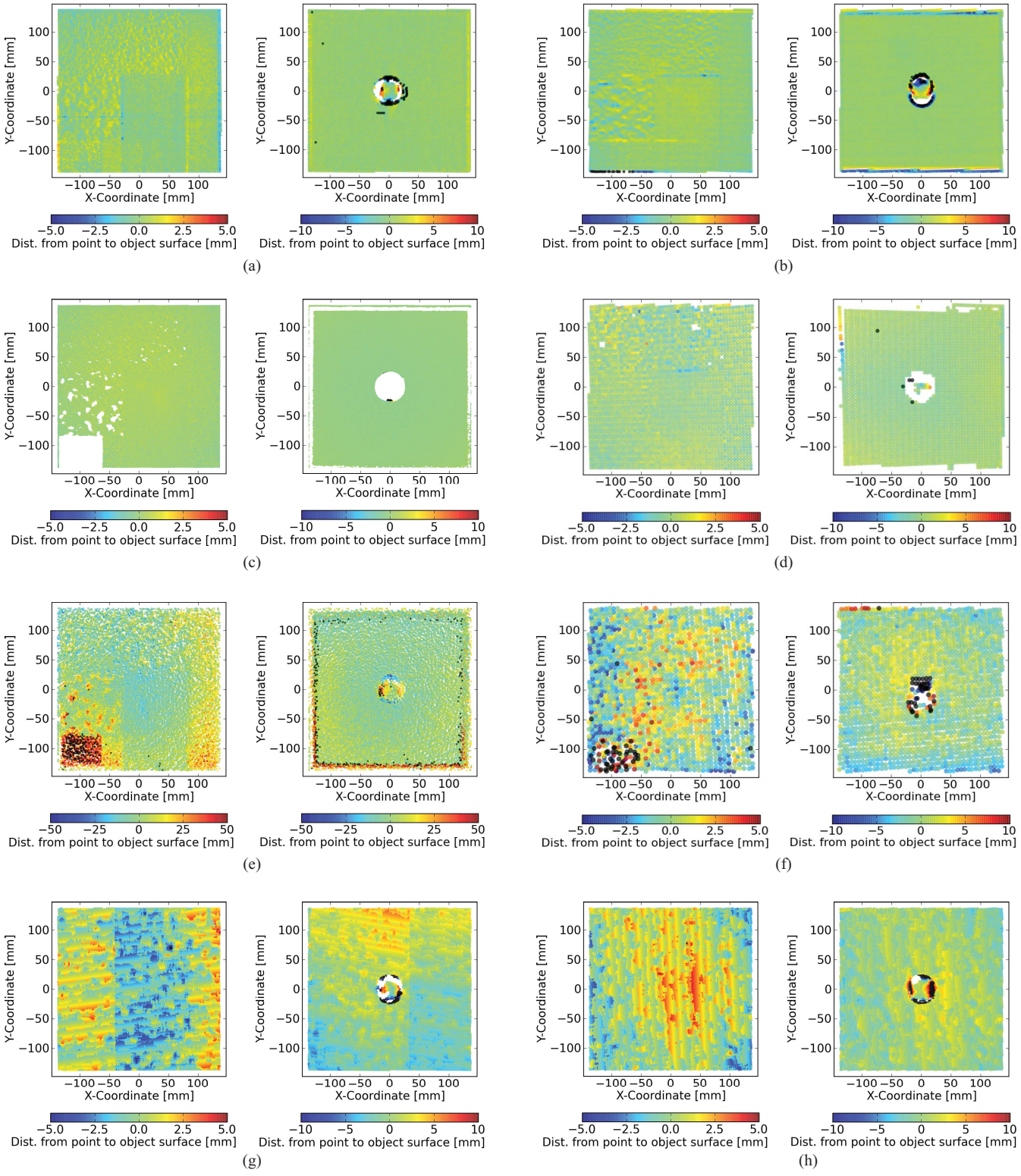

Fig. 9. Test results for front and back of test plate for each of the scanners that have been tested. All results shown here are for 320 lux ambient light. Black points symbolize distances outside error scale. (a) SICK Ranger 50E. (b) SICK Scanning Ruler. (c) 3D3 HDI Advance R2. (d) SCAPE Grid Scanner. (e) PMD CamCube 3.0 (increased error scale). (f) Fotonic C70. (g) Xbox Kinect. (h) ASUS Xtion PRO.

is only present in a very small region around the hemisphere. Hence, it seems like this scanner is eliminating some of the negative effects of specular reflections.

3) 3D3 HDI Advance R2: The results for the 3D3 HDI Advance R2 stripe pattern scanner are shown in Fig. 9(c). From this, it can be seen that no data could be detected in the

TABLE I

COMPARISON OF SELECTED RESULTS FROM TEST OF 3-D SENSORS. HARDWARE COSTS HAVE BEEN DIVIDED INTO THREE RANGES, LOW, MEDIUM, AND HIGH, WHERE LOW COVERS THE RANGE [0; 1000] EUROS, MEDIUM COVERS THE RANGE [1000; 8000] EUROS AND HIGH COVERS THE RANGE [8000; 15 000] EUROS[2]

Scanner @ 320 Lux Ambient Light	Front of Test Plate					Back of Test Plate		Hardware costs
	RMS Error in gray region	Max. RMS error in structured regions	Discretization			Fraction of points on hemisphere	RMS error on hemisphere top	
			Depth	In-plane 1	In-plane 2			
SICK Ranger 50E @ 2 m	0.5 mm	0.7 mm	0.3 mm	1.4 mm	2.8 mm	66%	0.9 mm	High[2]
SICK Scanning Ruler @ 1.5 m	0.3 mm	0.6 mm	0 mm	2.3 mm	2.4 mm	78%	1.2 mm	High
HDI Advance R2 @ 2.2 m	0.3 mm	0.3 mm	0 mm	0.6 mm	0.6 mm	5%	N/A	Medium
SCAPE Grid Scanner @ 60 cm	0.43 mm	0.7 mm	0 mm	5.0 mm	5.2 mm	21%	1.3 mm	Medium
PMD CamCube 3.0 @ 60 cm	9.1 mm	13 mm	0 mm	1.6 mm	1.9 mm	100%	12 mm	Medium
Fotonic C70 @ 90 cm	1.4 mm	1.5 mm	0.5 mm	6.0 mm	7.6 mm	65%	13 mm	Medium
Xbox Kinect @ 60 cm	1.2 mm	1.2 mm	2 mm	1.4 mm	1.4 mm	58%	1.7 mm	Low
ASUS Xtion PRO @ 60 cm	1.3 mm	1.1 mm	2 mm	1.4 mm	1.4 mm	90%	1.5 mm	Low
Scanner @ 140 Lux Ambient Light	Front of Test Plate					Back of Test Plate		
	RMS Error in gray region	Max. RMS error in structured regions	Discretization			Fraction of points on hemisphere	RMS error on hemisphere top	
			Depth	In-plane 1	In-plane 2			
SICK Ranger 50E @ 2 m	0.5 mm	0.6 mm	0.4 mm	1.4 mm	2.7 mm	66%	1.0 mm	
SICK Scanning Ruler @ 1.5 m	0.3 mm	0.6 mm	0 mm	2.3 mm	2.4 mm	83%	4.1 mm	
HDI Advance R2 @ 2.2 m	0.2 mm	0.2 mm	0 mm	0.6 mm	0.6 mm	35%	0.6 mm	
SCAPE Grid Scanner @ 60 cm	0.51 mm	0.6 mm	0 mm	4.9 mm	5.0 mm	16%	0.6 mm	
PMD CamCube 3.0 @ 60 cm	8.9 mm	12 mm	0 mm	1.6 mm	1.9 mm	98%	9.6 mm	
Fotonic C70	N/A	N/A	N/A	N/A	N/A	N/A	N/A	
Xbox Kinect @ 60 cm	1.2 mm	1.2 mm	2 mm	1.4 mm	1.4 mm	50%	1.7 mm	
ASUS Xtion PRO @ 60 cm	1.2 mm	1.1 mm	2 mm	1.4 mm	1.4 mm	73%	1.1 mm	

two darkest regions of the front of the test plate as well as some of the dark spots in the structured regions. This is because the light intensity of the standard projector used in this setup (Optoma TX536, 2800 ANSI lumens, 3000:1 contrast) is not sufficiently high relative to the intensity of the ambient light. The back of the test plate shows that although the scanner is not capable of scanning the shiny hemisphere, it is at least not affecting the surroundings of the test plate. Lowering the intensity of the ambient light to approximately 140 lux led to missing points only being present in the darkest region of the front of the test plate. Also, a small region with a radius of approximately half that of the hemisphere could be scanned on the hemisphere if lowering the intensity of the ambient light.

Quantitative comparison: An overview of selected results from the test of large 3D sensors can be seen in the first part of Table V-A.1. Generally, all three large scanners tested here perform quite well with RMS errors of points from the test plate of less than 1 mm. The HDI Advance scanner is almost unaffected by inhomogeneous surface intensities which can be seen by the fact that the RMS error is not increased from the gray region to the structured regions. Also, this scanner is able to deliver high density point clouds with a point-to-point distance of approximately 0.6 mm. The shortcomings of the illumination power of the projector is, however, evident from the two columns showing the results for the back of the test plate; virtually no points on the shiny hemisphere have been acquired. Lowering the intensity of ambient light to approximately 140 lux changed these two numbers to 35% and 0.6 mm, respectively.

In table V-A.1, the approximate hardware costs have also been included. These have been divided into three ranges; Low, Medium and High. See the caption for further details on these.

[2]The use of a SICK Ranger 50E requires that the scanner must be moved relative to the scanned scene by some external hardware, which is not included in this price.

B. Compact 3-D Sensors

As specified in section IV, compact 3D sensors have been tested at a distance of approximately 60 cm. These include the following five 3D sensors.

1) SCAPE Grid Scanner: The results for the SCAPE Grid Scanner static pattern scanner can be seen in Fig. 9(d). Looking at the results for the front of the test plate, it is visible that the Grid Scanner is slightly affected by the structured regions. These result in both 3D points with larger error and a few missing points.

The results for the back of the test plate show some outliers, both on the hemisphere as well as on the periphery.

One important issue, which is not visible from Fig. 9(d), is the unambiguous depth range which is particular for the Grid Scanner. For a nominal distance of 60 cm as in this test, all range data will be mapped to the [40; 80 cm] range, meaning that data originating from a surface which is e.g. 81 cm from the Grid Scanner will seem to be approximately 41 cm from the scanner. Hence, in order to use this 3D sensor, one must ensure that all data is in fact inside the unambiguous depth range.

2) PMD CamCube 3.0: The test results that were produced for the PMD CamCube 3.0 ToF-sensor at a distance of 60 cm were originally showing a test plate which was only 93% of the size of the actual test plate. Hence, data from this sensor needed to be scaled accordingly. The results after scaling can be seen in Fig. 9(e) where it should be noted that the range of the error data is much larger than the for all other sensors in order to better show the errors. This figure shows a large systematic error depending on the intensity of the surface which is scanned; dark regions appear to be closer to the sensor than bright regions. This topic has been discussed in [16], [17], [19] as a systematic error which a calibration of the ToF-sensor should be able to remove the effects of. The presence of these systematic errors in combination with

the fact that data needed to be scaled by approximately 7% indicates that the PMD CamCube 3.0 could use additional calibration before being usable in the range where it was tested.

3) Fotonic C70: The Fotonic C70 is another ToF-camera with a slightly lower resolution (160 × 120) than the CamCube 3.0, which has a resolution of 200 × 200 points. However, as can be seen in Fig. 9(f), the slightly lower resolution is compensated for by much more reliable data (notice the scale of errors), especially taking into account that this was acquired at a distance of 90 cm. The structured regions have a very low effect on the data quality and only in the darkest regions of the test plate is data too noisy to be usable. This degrading performance for darker regions is consistent with the general behavior of ToF-cameras as explained in section III-C.

Data for the back of the test plate shows that this scanner is, however, not performing well for shiny surfaces with very few and unreliable points being present on the shiny hemisphere and just outside it.

When comparing the data in the white region of the test plate for the Fotonic C70 as well as the PMD CamCube 3.0 with that for the first four 3D sensors, it can be seen that the RMS error for data from ToF-cameras is in general higher than for other 3D sensors, just as explained in section III-C.

4) Xbox Kinect: The results for the Kinect sensor can be seen in Fig. 9(g). There are several interesting things that can be observed from this figure. First of all, there is a step in the direction of the X-axis at approximately -40 and 40 mm in the scans of the front and back, respectively. These steps are no larger than the general depth discretization of approximately 2 mm but here, the step is at a fixed X-coordinate. The exact X-coordinate is, however, not fixed over time as described in [20], [21].

Another interesting fact is that the depth discretization of the Kinect is clearly visible from the steps in the direction of the Y-axis of approximately 2 mm. However, there seems to be some errors in addition to the depth discretization since the maximum deviation from the test plate is far above the [–1; 1 mm] range.[3]

Apart from these errors, the Kinect sensor does not seem to be influenced by the varying surface reflectance of the front of the test plate. Looking at the results for the back of the test plate, it is seen that the Kinect performs relatively well on shiny surfaces although the error quickly rises when moving away from the center of the hemisphere.

5) ASUS Xtion PRO: The results for the ASUS Xtion PRO are shown in Fig. 9(h). From this, it is clearly visible that this sensor is built on the same technology as the Kinect since the results are more or less the same as those in Fig. 9(g). The vertical lines from Fig. 9(g) are, however, not present but whether this is because this issue has been fixed for the Xtion PRO sensors is not known.

[3]It should be noted that according to [22], the nominal working range of the Kinect 3D sensor is 0.5 to 5.0 m, meaning that it has been tested at the edge of its nominal working range. If testing at larger distances, the depth discretization as well as depth errors are expected to increase [21], [22].

Quantitative comparison: Selected results for the compact sensors that have been tested can be seen in the second part of Table V-A.1. In this, the PMD CamCube 3.0 stands out as the sensor with the worst test results. If averaging range data over 20 frames from the CamCube, the RMS error in the gray region decreases to 4.3 mm, a reduction of 53% whereas the maximum RMS error in the structured regions only decreases to 9.8 mm, a reduction of 25%. This clearly shows the systematic errors arising from the structured regions.

On the matte surfaces, the remaining four compact sensors perform relatively similarly with the Grid Scanner having the lowest RMS error and the Kinect and the Xtion having the largest point densities. It should be noted that point densities close to that of the CamCube are achievable with a Fotonic C40 if scanning at the same distance of 60 cm since it has a FoV of ±20° horizontally in comparison to the C70, which has a FoV of ±35° horizontally.

When looking at the results for the shiny surface, it can be seen that the scanners giving the most reliable data from this are the Kinect and the Xtion. These have both succeeded in generating 3D points which are very close to the actual surface on a relatively large part of the hemisphere.

The only parameter where the Kinect and Xtion perform poorly is in the depth discretization, which has also been described in, e.g., [20]. For some applications, this might not be an issue but for some high precision purposes, e.g. quality control, a depth discretization of 2 mm at a distance of 60 cm might be insufficient.

VI. Conclusion

In this work, a test procedure for 3D scanners has been described. This procedure involves scanning a test plate which has been developed for this test. The test plate has been designed to make it possible to evaluate the real-world performance of the scanners that are subject to testing. Also, the test plate had been made mobile, making it practically possible to test several different 3D scanners.

Using this test procedure, eight different scanners have been tested and evaluated upon.

Determining which of these 3D scanners is optimal depends on the application for which it is to be used. For high precision tasks, the SICK Ranger 50E and the SICK Scanning Ruler are both optimal choices but for applications where the sensitivity to ambient light is of no concern, the HDI Advance R2 may be a cost effective alternative with even higher point densities and lower RMS errors.

If reliable 3D data from both matte and shiny surfaces is required and the point density is of lower importance, the SCAPE Grid Scanner is a good choice, assuming that the limited depth range of this scanner is acceptable. If, however, slightly lower data quality is required, both the Fotonic C70/C40 as well as the Xbox Kinect and the ASUS Xtion PRO sensors should be adequate choices, depending on the allowable price range.

ACKNOWLEDGMENT

The authors would like to thank F. Nilsson from SICK IVP in Linköping, Sweden, K. Wong from 3D3 Solutions in Burnaby, BC, Canada, G. Forsén from Fotonic in Stockholm, Sweden, and I. Schwengber from PMDTechnologies in Siegen, Germany, for helping with scanning the test plate and delivering data for this paper.

REFERENCES

[1] R. Palaniappan, P. Mirowski, T. K. Ho, H. Steck, P. Whiting, and M. MacDonald, "Autonomous RF surveying robot for indoor localization and tracking," in *Proc. Int. Conf. Indoor Position. Indoor Navigat.*, Guimarães, Portugal, Sep. 2011, pp. 1–4.

[2] K. Wolf, D. Roller, and D. Schäfer, "An approach to computer-aided quality control based on 3D coordinate metrology," *J. Mater. Process. Technol.*, vol. 107, no. 1, pp. 96–110, Nov. 2000.

[3] A. Georgopoulos, C. Ioannidis, and A. Valanis, "Assessing the performance of a structured light scanner," *Int. Archives Photogram., Remote Sensing Spatial Inf. Sci.*, vol. 38, no. 5, pp. 250–255, Jun. 2010.

[4] J.-A. Beraldin and M. Gaiani, "Evaluating the performance of close range 3D active vision systems for industrial design applications," *Proc. SPIE, Electron. Imag.*, vol. 5665, pp. 67–77, Jan. 2005.

[5] W. Shackleford and R. Bostelman, "Data collection test-bed for the evaluation of range imaging sensors for ANSI-ITSDF B56.5 safety standard for guided industrial vehicles," in *Proc. 9th Workshop Perform. Metrics Intell. Syst.*, Gaithersburg, MD, Sep. 2009, pp. 155–160.

[6] G. Guidi and F. Remondino, "Performances evaluation of a low cost active sensor for cultural heritage documentation," in *Proc. 8th Conf. Opt. 3-D Meas. Tech.*, vol. 2. Zurich, Switzerland, 2007, pp. 59–69.

[7] M. Russo, G. Morlando, and G. Guidi, "Low cost characterization of 3D laser scanners," *Proc. SPIE, Electron. Imag.*, vol. 6491, pp. 7.1–7.9, Jan. 2007.

[8] G. Guidi, F. Remondino, M. Russo, and A. Spinetti, "Range sensors on marble surfaces: Quantitative evaluation of artifacts," *Proc. SPIE, Videometrics, Range Imag., Appl.*, vol. 7447, pp. 3.1–3.12, Aug. 2009.

[9] J. Clark and S. Robson, "Accuracy of measurements made with a Cyrax 2500 laser scanner against surfaces of known colour," *Int. Archives Photogram., Remote Sensing Spatial Inf. Sci.*, vol. 35, no. 4, pp. 1031–1036, Jul. 2004.

[10] T. Luhmann, "Comparison and verification of optical 3-D surface measurement systems," *Int. Archives Photogram., Remote Sensing Spatial Inf. Sci.*, vol. 37, no. 5, pp. 51–56, Jul. 2008.

[11] B. Ravani, "Creating standards and specifications for the use of laser scanning in caltrans projects," AHMCT, Davis, CA, Res. Rep. UCD-ARR-07-06-30-01, Jun. 2007.

[12] W. Boehler, M. B. Vicent, and A. Marbs, "Investigating laser scanner accuracy," in *Proc. 19th Int. Sci. Committee Document. Cultural Heritage Symp.*, Antalya, Turkey, Sep.–Oct. 2003, pp. 1–9.

[13] P. Nilsson, "3D-vision guided robotics for material handling," in *Proc. 41st Int. Symp. Robot.*, Jun. 2012, pp. 1–7.

[14] C. Rocchini, "A low cost 3D scanner based on structured light," in *Proc. Eurograph.*, vol. 20. Manchester, U.K., Sep. 2001, pp. 1–6.

[15] A. Blake, "Three-dimensional vision system," U.S. Patent 3 003 579, Feb. 18, 1993.

[16] S. Fuchs and G. Hirzinger, "Extrinsic and depth calibration of ToF-cameras," in *Proc. 26th IEEE Conf. Comput. Vis. Pattern Recognit.*, Anchorage, AK, Jun. 2008, pp. 1–6.

[17] T. Kahlmann, F. Remondino, and H. Ingensand, "Calibration for increased accuracy of the range imaging camera Swissranger," in *Proc. Int. Soc. Photogram. Remote Sensing Commission V Symp.*, vol. 36. Dresden, Germany, Sep. 2006, pp. 1–6.

[18] S. May, "3D pose estimation and mapping with time-of-flight cameras," in *Proc. IEEE/RSJ Int. Conf. Intell. Robots Syst., Workshop 3D-Mapping*, Nice, France, Sep. 2008, pp. 1–6.

[19] S. Oprisescu, D. Falie, M. Ciuc, and V. Buzuloiu, "Measurements with ToF cameras and their necessary corrections," in *Proc. Int. Symp. Signals, Circuits Syst.*, vol. 1. Iasi, Romania, Jul. 2007, pp. 221–224.

[20] J. Smisek, M. Jancosek, and T. Pajdla, "3D with kinect," in *Proc. 13th Int. Conf. Comput. Vis.*, Barcelona, Spain, Nov. 2011, pp. 1–8.

[21] S. M. Olesen, S. Lyder, J. B. Jessen, and N. Krüger, "Real–time extraction of surface patches with associated uncertainties by means of kinect cameras," *J. Real-Time Image Process.*, Jul. 2012.

[22] K. Khoshelham, "Accuracy analysis of kinect depth data," in *Proc. Int. Soc. Photogram. Remote Sensing, Workshop Laser Scan.*, vol. 38. Calgary, AB, Canada, Aug. 2011, pp. 1–10.

Bent Møller, photograph and biography are not available at the time of publication.

Ivar Balslev, photograph and biography are not available at the time of publication.

Norbert Krüger, photograph and biography are not available at the time of publication.